BNL-79248-2007-BC

Role of C and P sites on the Chemical Activity of Metal Carbide and Phosphides: From Clusters to Single-Crystal Surfaces

José A. Rodriguez[a] , Francesc Viñes[b], Ping Liu[a] and Francesc Illas[b]

[a]Department of Chemistry, Brookhaven National Laboratory, USA
[b] Departament de Química Física, Universitat de Barcelona, Spain

To be published in "Model Systems in Catalysis: From Single Crystals and Size-Selected Clusters to Supported Enzyme Mimics"

July 2007

Chemistry Department

Brookhaven National Laboratory
P.O. Box 5000
Upton, NY 11973-5000
www.bnl.gov

DISCLAIMER

BNL-79248-2007-BC

Role of C and P Sites on the Chemical Activity of Metal Carbide and Phosphides: From Clusters to Single-Crystal Surfaces

José A. Rodriguez[a] , Francesc Viñes[b], Ping Liu[a] and Francesc Illas[b]

[a]Department of Chemistry, Brookhaven National Laboratory, USA
[b] Departament de Química Física, Universitat de Barcelona, Spain

Abstract

Transition metal carbides and phosphides have shown tremendous potential as highly active catalysts. At a microscopic level, it is not well understood how these new catalysts work. Their high activity is usually attributed to ligand or/and ensemble effects. Here, we review recent studies that examine the chemical activity of metal carbide and phosphides as a function of size, from clusters to extended surfaces, and metal/carbon or metal/phosphorous ratio. These studies reveal that the C and P sites in these compounds cannot be considered as simple spectators. They moderate the reactivity of the metal centers and provide bonding sites for adsorbates.

Keywords: Metal carbides, Metal phosphides, Catalysis, Hydrocarbon transformations, Desulfurization

I. Introduction

The carbides of the early-transition metals exhibit chemical and catalytic properties that in many aspects are very similar to those of expensive noble metals [1]. Typically, early-transition metals are very reactive elements that bond adsorbates too strongly to be useful as catalysts. These systems are not stable under a reactive chemical environment and exhibit a tendency to form compounds (oxides, nitrides, sulfides, carbides, phosphides). The inclusion of C into the lattice of an early-transition metal produces a substantial gain in stability [2]. Furthermore, in a metal carbide, the carbon atoms moderate the chemical reactivity through ensemble and ligand effects [1-3]. On one hand, the presence of the carbon atoms usually limits the number of metal atoms that can be exposed in a surface of a metal carbide (ensemble effect). On the other hand, the formation of metal-carbon bonds modifies the electronic properties of the metal (decrease in its density of states near the Fermi level; metal→carbon charge transfer) [1-3], making it less chemically active (ligand effect) and a better catalyst according to the Sabatier's principle [2]. Thus, the carbides of early-transition metals are able to catalyze the transformation of hydrocarbons [1,4], the conversion of methane to synthesis gas [5,6], and desulfurization reactions [1,7-12]. In broad terms, these compounds display a unique combination of the physical properties characteristic of noble metals and ceramics [13,14]. Many early-transition metal carbides are good electrical and thermal conductors while possessing ultra-hardness and very high melting points [13,14]. All these chemical and physical properties make the early-transition metal carbides useful for technological applications in catalysis and materials science [1,13,14].

The inclusion of P into the lattice of an early-transition metal also leads to a substantial gain in stability [2]. In general, the metal-P bonds are less ionic than metal-C bonds and the ligand effects of P are not very strong [2,15]. This may be important for some catalytic reactions, like

hydrodesulfurization processes [15]. An important issue when dealing with metal-carbide and metal–phosphide catalysts is the role of the light elements (C and P) in catalytic processes. Are the light elements simple spectators, as it is frequently assumed [1,7,9], or participate directly in the reactions which are being catalyzed? In this chapter we review a series of recent studies that focus on the chemical and catalytic properties of metal carbides and phosphides. Many of these studies have been performed on well-defined single crystal surfaces. A few of them deal with nanoparticles such as the metcars Ti_8C_{12} or Mo_8C_{12} (see Figure 1). The chapter is organized as follows. The next section examines the effects of the carbon/metal ratio on the electronic properties and chemical reactivity of metal carbides. Then, we report systematic studies for the adsorption of oxygen on metal carbides. In the last part of the chapter, we end with studies of desulfurization on metal carbides and phosphides. In recent years new legislations require a very low content of sulfur in oil-derived products and new catalysts have been developed for deep hydrodesulfurization reactions which are based of metal carbide and phosphide compounds (1,9,15).

II. Effects of carbon/metal ratio on the chemical properties of metal carbides.

Since Boudart et al. found that early transition metal carbides behave like noble metals in surface catalysis [4], this class of materials has attracted considerable attention [1]. Computational

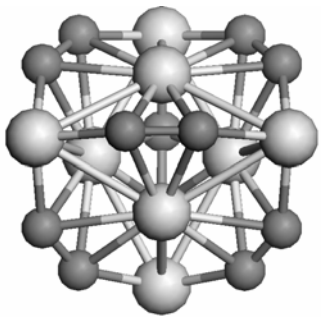

Fig 1 Calculated structure for metcar nanoparticles, M_8C_{12} (M=Ti,V,Mo). Large grey spheres denote metal atoms, small dark spheres represent C atoms (taken from ref [8]).

methods based on functional (DF) theory were employed to study the stabilities and chemical activities of transition metal carbides [3,8,12]. Different kinds of structures including bulk surfaces —$M_2C(001)$ and $MC(001)$ (see Figure 2)— and metcars, M_8C_{12} (Figure 1; M= Ti, V or Mo), were taken into consideration [16]. Systematic studies show that by raising the C coordination number of the metal atoms in the carbides, in general the stability of the carbides increases (metcars are an exception since they include both high-coordinated and low-coordinated metal atoms.); at the same time, the chemical activities of the carbides decrease due to a downshift of the metal d-band center (ligand effect) [8].

Figure 3 displays calculated bonding energies for CO, S, SO_2 and thiophene on a series of carbide surfaces and metcars [16]. It is usually assumed that the chemical activity of the metal carbides decreases when raising the C concentration [1]. This hypothesis is not supported by the DF results in Figure 3: the activity of the carbides follows a volcano-like curve with the increasing carbon/metal (C/M) ratio. The metcar nanoparticles have a chemical reactivity much higher than expected for their large C/M ratio of 1.5.

CO is a molecule frequently used to probe chemical reactivity. With the C/M ratio increasing up to 1, the CO adsorption energy on the surfaces from M(001) to MC(001) decrease

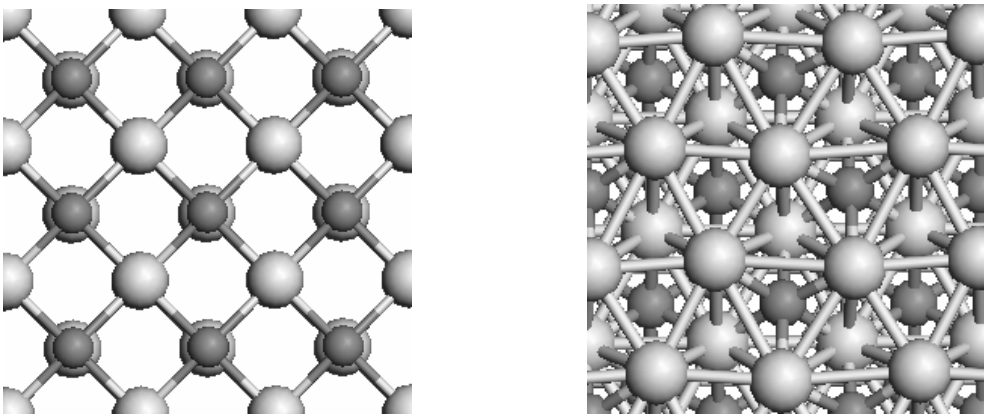

Fig 2 Left: Top view for the (001) face of MC carbides (M= Ti, V, Zr, or Mo). Right: Top view of the $Mo_2C(001)$ surface (taken from ref. [8]). Large spheres represent metals.

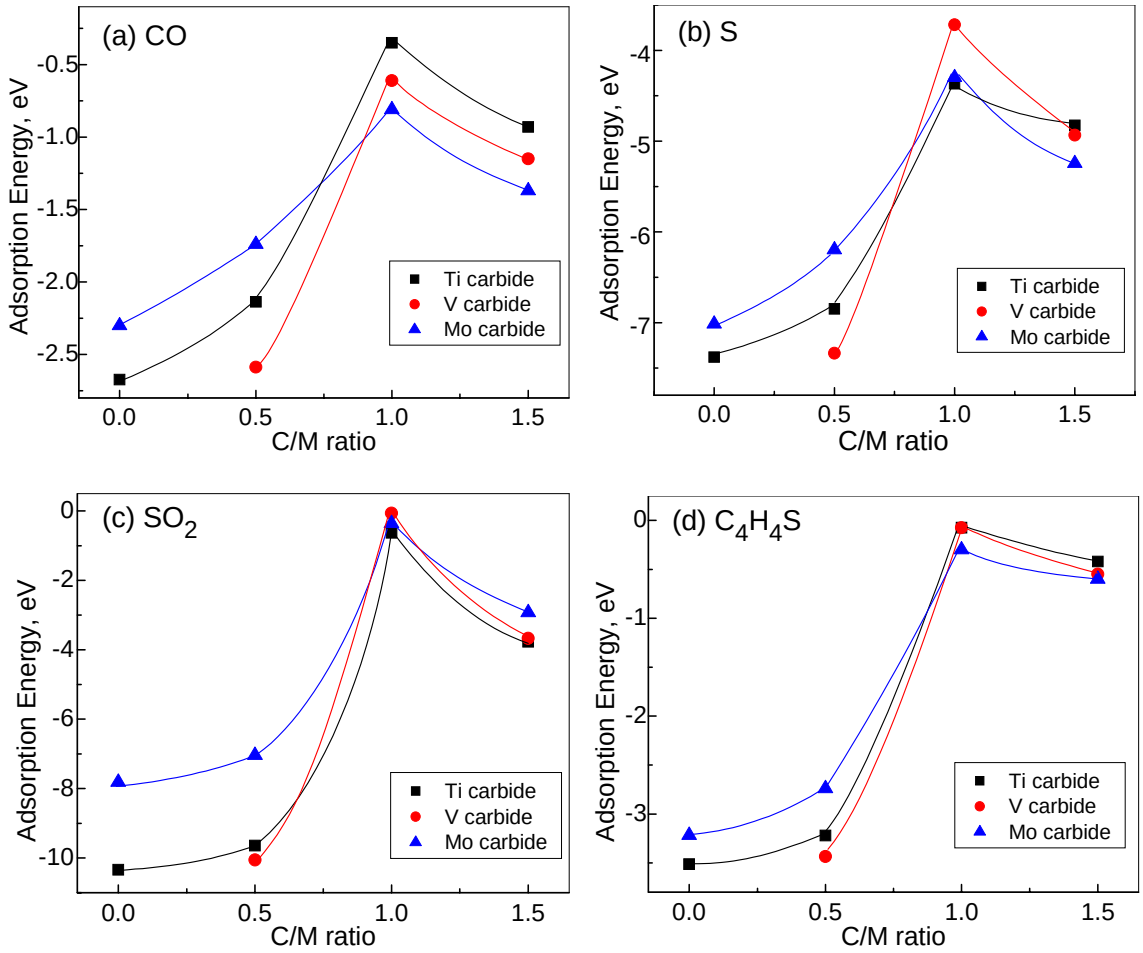

Figure 3 Calculated adsorption energies of carbon monoxide (a), atomic sulfur (b), sulfur dioxide (c) and thiophene (d) on the metal carbides (Ti carbides, V carbides and Mo carbides) as a function of the C/M ratio. The C/M values of 0.5, 1 and 1.5 correspond to bulk M_2C, bulk MC, and metcar M_8C_{12}, respectively (taken from ref. 16).

greatly by ~ 2 eV (Figure 3a). However, the CO-M bonds become stronger by ~0.5 eV when increasing the C/M ratio to 1.5 and forming M_8C_{12} nanoparticles. In spite of the high C/M ratio and the C_2 groups (Figure 1), M_8C_{12} displays a much stronger interaction with CO than that of MC (Figure 3a). As shown in Figures 3b-d, the variation of the adsorption energy for S, SO_2 and tiophene with the C/M ratio displays a similar volcano trend as that seen in Figure 3a. Considering the best catalysts those that combine high stability and moderate chemical activity, the DF results suggest that the catalytic potential of Mo carbide systems should decrease in the following sequence: Mo_8C_{12} > $Mo_2C(001)$ or $MoC(001)$ > pure Mo(110). In spite of having the

largest C/Mo ratio, the metcar appears as the most attractive system [8,12]. The theoretical studies also indicate that the "magic" behavior of metcars is not unique for Mo carbides. Similar behavior is also observed for Ti or V carbides [8,16]. As we will see in section IV, the metcars are more efficient catalysts for the hydrodesulfurization of thiophene than Mo_2C(001) or MoC(001) [17].

III. Reaction of oxygen with metal carbide surfaces

The interaction of oxygen with surfaces of metal carbides is a very important issue [1]. The catalytic properties of metal-carbides can be drastically modified by adsorption of oxygen from the air or by reaction with O centers of oxide supports [1,18]. In addition, oxygen also affects the performance of metal-carbide coatings used in the fabrication of mechanical and electronic devices [13,14,19]. The generation of an oxide film on top of the carbide can lead to a degradation of the conductivity and hardness of the system [13,14], and oxocarbides can have interesting physical properties on their own [1,18]. Several experimental studies have investigated the interaction of oxygen with well-defined surfaces of metal carbides [19-24]. A key point is the relative importance of the oxygen↔metal and oxygen↔carbon interactions. Usually, it is assumed that the C sites of a metal carbide surface play a secondary or minor role in the chemical properties of the system [1,7,9]. However, recent experimental studies for O/TiC(001) and ZrC(001) point to the existence of strong oxygen↔carbon interactions [19,23,24].

High-resolution photoemission and first-principles DF calculations were used to study the interaction of oxygen with TiC(001), ZrC(001) and VC(001) surfaces [23,24]. Atomic oxygen is present on the carbide substrates after small doses of O_2 at room temperature. At 500 K, the oxidation of the surfaces is fast and clear features for TiO_x, ZrO_x or VO_x are seen in core-level

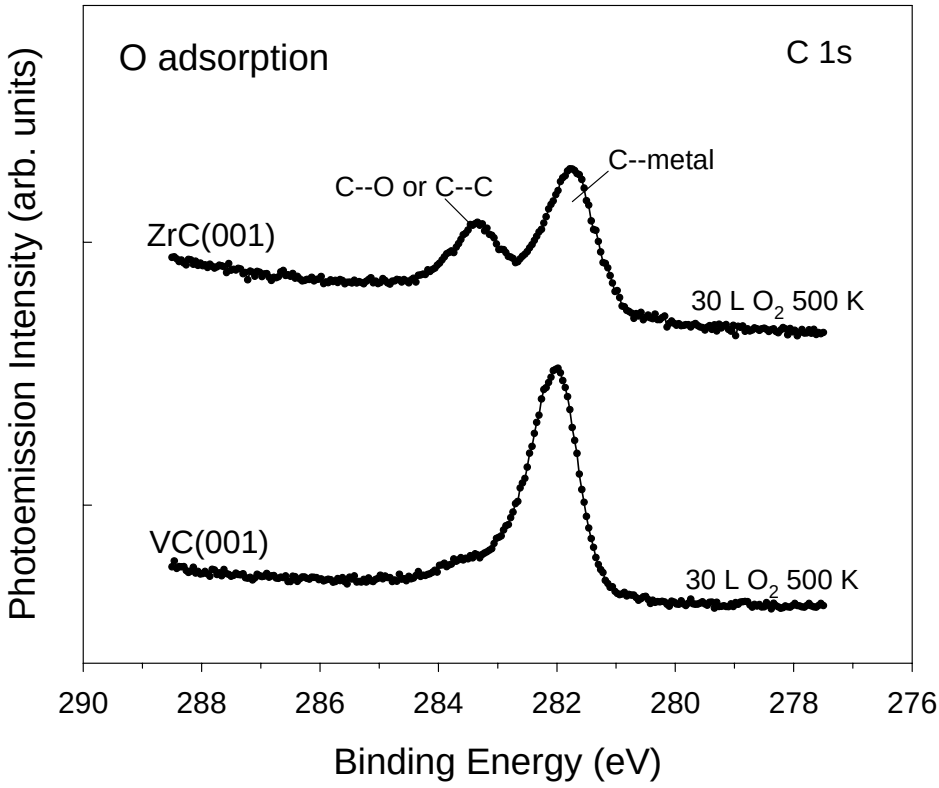

Figure 4. C 1s photoemission spectra recorded after doing oxygen to ZrC(001) and VC(001) at 500 K (taken from ref. 24).

photoemission. Figure 4 shows high-resolution C 1s photoemission spectra for O/ZrC(001) and O/VC(001) surfaces. The C 1s spectrum for O/ZrC(001) exhibits a distinctive line shape with two strong peaks at 283.4 and 281.9 eV. The peak at 281.9 eV is close in binding energy to the single peak found for clean ZrC(001) at 281.7 eV. From the relative intensities of the two peaks it appears that, in O/ZrC(001), a very large fraction (~ 40 %) of the C atoms near the surface has been perturbed by the presence of oxygen. In general, we found C 1s shifts of 1.3-1.6 eV with respect to the main peak for the substrate. Similar results have been found for O/TiC(001) [23]. They point either to a strong interaction between O and C atoms (oxygen could be adsorbed directly on top of C sites) or to a O↔C exchange which could take place in the surface (Zr-C or

TiC bonds being replaced by Zr-O or Ti-O and C-C bonds). These two possibilities were investigated using DF calculations [23,24]. The calculations show a CZrZr or CTiTi pseudo-hollow as the most stable site for the adsorption of O on ZrC(001) or TiC(001), see Figure 5. Furthermore, the calculations also show that a C↔O exchange is exothermic on these metal carbide substrates, and the displaced C atoms bond to CZrZr sites or CTiTi sites. Thus, in the O/ZrC(001) and O/TiC(001) systems, the surface C atoms play a major role in determining the behavior of the system [23,24].

In Figure 4, the C 1s spectrum for O/VC(001) is characterized by essentially a single peak at 282.1 eV and a very small feature near 283.5 eV. For clean VC(001), the C(1s) peak shows up at 282.0 eV. Thus, it appears that the O↔C interactions are negligible in O/VC(001). The results of photoemission are consistent with data of HREELS for O/VC(001) [19]. The C(1s) spectra in Figure 4 suggest a big difference in the mechanisms for the oxidation of ZrC(001) and VC(001). First-principles DF calculations corroborate this finding [24,25]. For the interaction of oxygen

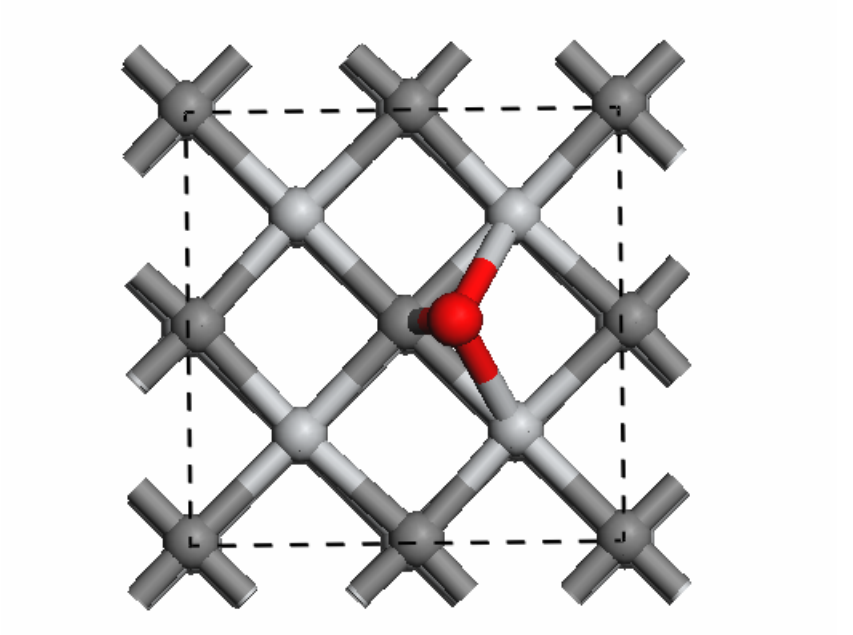

Fig 5 Calculated adsorption site for O on TiC(001) and ZrC(001). Dark grey spheres represent C atoms, while metal atoms are represented by soft grey spheres (taken from ref. 24).

with the VC(001) surface, the DF calculations show no big differences for the O adsorption energies on top of V and on a CVV hollow [24,25]. However, the calculated rate constant for the dissociation of O_2 on V sites is much larger than that on CVV sites [25], and from this one may deduce that the O↔C interactions are not really essential for the binding of the adsorbate in O/VC(001). The VC(001) valence band has one more electron than that of TiC(001) or ZrC(001) [3], and it occupies states that favor V-O bonding and the dissociation of molecular oxygen [24,25].

Density functional calculations were used to perform a systematic study of the adsorption of atomic O and O_2 on the (001) surface of a series of transition metal carbides (TMC, TM=Ti, Zr, Hf, V, Nb, Ta, Mo) [26,27]. On group 4 TMCs, oxygen atoms highly preferred the hollow sites surrounded by one carbon atom and two metal atoms (CMM, see Figure 5). On the rest of TMCs for groups 5 and 6 a competition between this site and the O adsorption on top of a metal atom (M-top) was observed. A third possible competitive minimum was found for the δ-MoC(001) system, where a kind of CO-like molecule was formed and adsorbed on the carbon vacancy site. The strong interaction of O with the C explains the availability of carbon removal and formation of metal oxycarbide compounds by oxidation, especially at high temperatures [26].

A topological analysis of the electron localization function (ELF) provides an unbiased description of the chemical bond [28]. The ELF contours for O adsorption on the M-top site are reported on Figure 6 for a representative TMC of groups 4, 5 and 6 of the Periodic Table. These results do not exhibit any region with a large value of ELF between the adsorbate and the surface and hence there is no evidence of either covalent or metallic bonding, the electron pairs are all

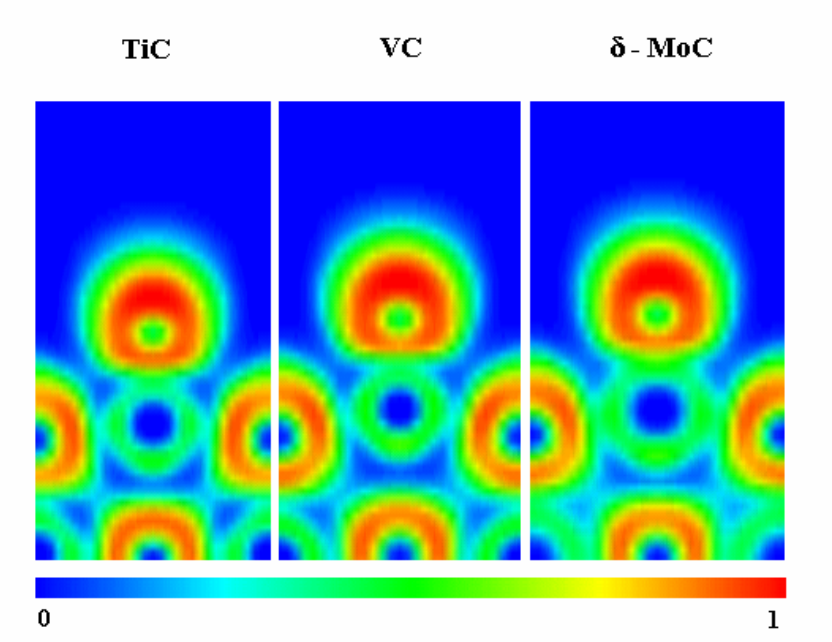

Fig 6 Electron localization function (ELF) maps for the adsorption of O on M-top sites of TiC(001), group 4 of the Periodic Table, VC(001), group 5, and δ-MoC(001), group 6 (taken from ref. [26]).

well localized over the oxygen atoms as expected for a dominantly ionic bond. The plots show a weaker bonding interaction for oxygen on Ti than on V or Mo. For the interaction of atomic O above the CMM adsorption site (not shown), a well defined basin with a high ELF contour between the oxygen adatom and the surface carbon was clearly observed [26], indicating significant covalent bonding at this site. An analysis of the partial density-of-states near the Fermi level, Mulliken charges, and adsorbate-induced work function changes point to adsorption bonds which contain a strong mixture of ionic and covalent character [23,24,26].

In a DF study for the adsorption and dissociation of O_2 on the (001) surface of group 4-6 TMCs [27], it is found that O_2 may adsorb molecularly on two different substrate sites with similar adsorption energy. At these sites, O_2 either bridges two surface M atoms or it is placed directly on top of a M surface atom. A case apart is δ-MoC(001), where O_2 adsorption on-top of surface Mo atoms is far up in energy with respect to bridging two surface Mo atoms. The relative

stability of O_2 on these TMCs is dominated by the electron back-donation between the surface and O_2 and the stabilization of the resulting partially charged molecule by the surface metal sites. Three reaction paths leading to O_2 dissociation were considered [27]. The first reaction pathway starts from M-M bridge molecular adsorption and lead to O atoms on-top of surface M atoms (TS^M), the second one (TS^C) starts from on-top molecular adsorption and leads to final states where O atoms are adsorbed on three-fold hollow sites neighboring two M and one C surface atoms, while the third pathway (TS^{BC}) starts from O on the M-M bridge and leads to TS^C products. For each reaction path, transition state structures have been located and the corresponding energy barriers obtained [27]. At low temperatures, O_2 dissociation on group 4 TMCs can only occur via the TS^{BC} pathway whereas at high temperatures it may also take place starting through TS^C. For the rest of the carbides, only TS^C and TS^M paths are possible. The calculated transition state theory rate constants reveal that TMCs of groups 4 and 5 are easy to oxidize whereas this is especially difficult for δ-MoC(001).

The calculated ΔE's for the formation of oxycarbides indicate that two reaction paths are possible for the C↔O exchange in O/TiC(001) or O/ZrC(001) [23,24]:

$$O/MC(001) \rightarrow C/MC_{1-x}O_x(001) \quad (1)$$

$$O/MC(001) \rightarrow MC_{1-x}O_x(001) + CO(gas) \quad (2)$$

Reaction (1) essentially involves one oxygen atom per each carbon atom and does not change the C content of the system. The C atoms replaced by O remain on the surface bonded to CMM sites, see Figure 7 [23,24]. In the case of Reaction (2), the carbon content of the system decreases. It involves two O atoms per each C atom removed. One O atom takes the place of a C atom in the carbide lattice, and the second O atom reacts with the replaced C to form CO which evolves into gas phase. For O/VC(001), DF calculations predict that a simple C↔O exchange is endothermic,

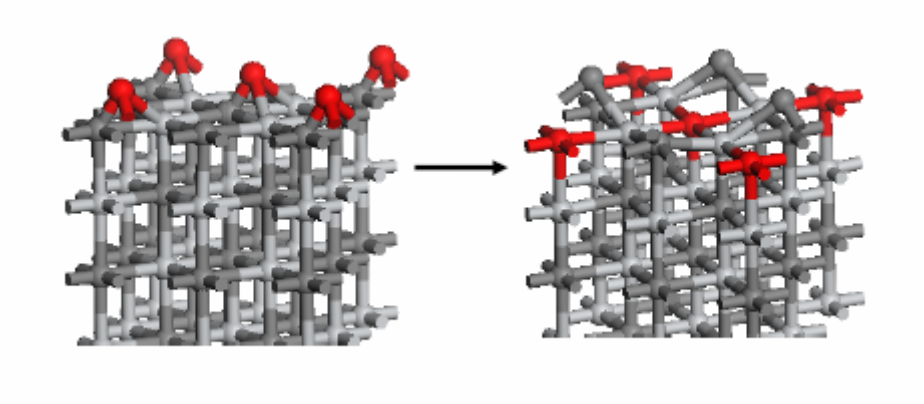

Figure 7. O/MC(001)→C/$MC_{1-x}O_x$(001) exchange on a metal carbide surface. The carbon atoms are represented by dark grey spheres, while the soft grey spheres denote metal atoms (taken from ref. [24]).

and only Reaction (2) is allowed thermodynamically [24].

IV. Desulfurization reactions on metal carbides and phosphides

Since the last century petroleum has been a very important source of fossil fuels and chemical feedstocks. Sulfur-containing compounds are common impurities in all crude oil [7,9]. In our industrial society, these impurities have a negative impact in the processing of oil-derived chemical feedstocks and degrade the quality of the air by forming sulfur oxides (SO_x) during the burning of fuels and by poisoning the catalysts used in vehicle catalytic converters [29]. Hydrodesulfurization (HDS) is one of the largest processes in petroleum refineries where sulfur is removed from the crude oil [7,9,29]. Organosulfur compounds are converted to H_2S and hydrocarbons by reaction with hydrogen over a catalyst. Most commercial HDS catalysts contain a mixture of MoS_2 and Ni or Co [7,30]. The current HDS catalysts cannot provide fuels with the low content of sulfur required by new environmental regulations [9,30]. The search for better desulfurization catalysts is a major issue nowadays in industry and academic institutions [15,29,30]. Thus, it has been established that β-Mo_2C and other metal carbides are very active for the cleavage of C-S bonds, but their HDS activity decreases quickly with time [31]. The

degradation of β-Mo_2C has been ascribed to the formation of a chemisorbed layer of sulfur or MoS_xC_y compounds on the surface of the catalyst [31]. More recently, transition metal phosphides have shown a tremendous potential as highly active HDS catalysts [9,32,33]. Among all the phosphides, Ni_2P/SiO_2 demonstrated the highest HDS activity (HDS conversion of 99%) and has been reported to be more efficient than $NiMoS/Al_2O_3$ (HDS conversion of 76%) [9,32]. Furthermore, Ni_2P does not deactivate with time as β-Mo_2C does [33].

X-ray photoelectron spectroscopy and first-principles DF calculations were used to investigate the desulfurization of thiophene (a typical test molecule in HDS studies) and the removal of S on surfaces of Ni_2P, Mo_2C and MoC [15]. The $Ni_2P(001)$ surface studied exposes both Ni and P sites, see Figure 8. This surface is of great relevance because is the predominant orientation observed in HDS catalysts containing Ni_2P crystallites on a silica support [31]. It has well-defined ensembles of three metal atoms that are separated by ~ 3.8 Å [34]. Each cluster of nickel is surrounded by a group of six P atoms. In contrast, an α-$Mo_2C(001)$ surface exposes only metal atoms (Figure 2) [11,12]. This carbide surface is expected to have a chemical reactivity very similar to that of a metal surface [2].

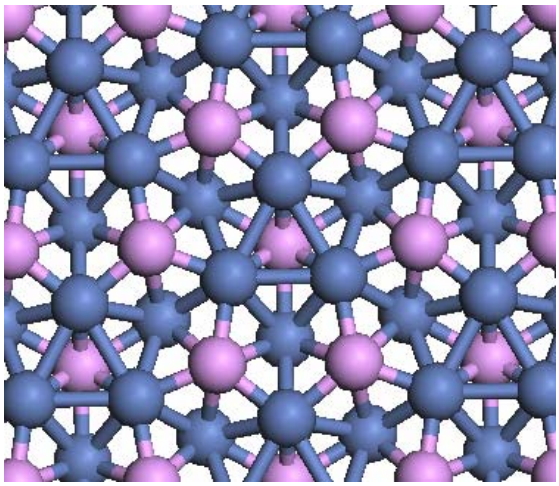

Figure 8 Structure of the $Ni_2P(001)$ surface. The dark blue spheres denote Ni atoms, P atoms are represented by soft purple spheres (taken from ref. [15]).

Thiophene (C_4H_4S) was dosed to $Ni_2P(001)$, α-$Mo_2C(001)$ and MoC surfaces at 100 or 300 K [15]. Figure 9 shows S 2p XPS spectra acquired after dosing the molecule at room temperature. For chemisorbed thiophene, the S 2p features are expected at 167-164 eV. The position of the S 2p features seen for the $C_4H_4S/Ni_2P(001)$ and C_4H_4S/α-$Mo_2C(001)$ systems, 164-160 eV, is typical of sulfur adatoms [15] indicating cleavage of the C-S bonds in thiophene. In contrast, the molecule does not dissociate or adsorb on MoC at 300 K. Photoemission data for C_4H_4S/α-$Mo_2C(001)$ show that C-S bond scission occurs by 170 K and possibly at temperatures as low as 105 K upon adsorption [11]. DF calculations also find a very strong interaction between C_4H_4S and α-$Mo_2C(001)$ [12]. The molecule adsorbs with its ring parallel to the carbide surface, and one of the C-S bonds spontaneously breaks. In contrast, theoretical studies shown weak bonding interactions for thiophene on a flat δ-MoC(001) surface [12]. A Mo→C charge transfer (ligand effect) and a dilution in the fraction of metal atoms in the surface (ensemble effect) make δ-MoC(001) inert towards thiophene. Experimental results for C_4H_4S/MoC confirm this theoretical prediction [15]. Thiophene adsorbs on polycrystalline MoC at 100 K, and

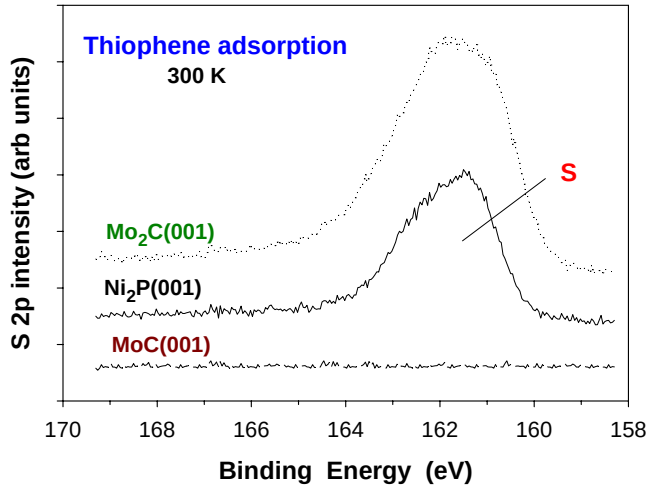

Figure 9 S 2p XPS spectra recorded after the adsorption of thiophene on $Mo_2C(001)$, $Ni_2P(001)$ and MoC at 300 K (taken from ref. [15]).

desorbs intact upon heating to 200 K. From TPD experiments, a thiophene adsorption energy of ~ 11 kcal/mol (0.48 eV) is estimated, which is close to the value of 7 kcal/mol (0.3 eV) calculated for C_4H_4S on a flat δ-MoC(001) surface [12,15].

In the case of $Ni_2P(001)$, the Ni→P charge transfer is not large (< 0.1 e) [15] and the surface has a substantial number of Ni atoms. Clusters of three Ni atoms are present (Figure 8), and the separation between these clusters is not large enough to prevent effective bonding interactions with a relatively big molecule like thiophene. At 100 K molecular adsorption of C_4H_4S on $Ni_2P(001)$ occurs, but at temperatures above 200 K the surface is able to crack the C-S bonds of the adsorbate [15]. Similar results have been found for the interaction of thiophene with Ni_2P/SiO_2 catalysts [32].

Thus, it is clear that both α-$Mo_2C(001)$ and $Ni_2P(001)$ can dissociate thiophene easily. The key to establish a catalytic cycle for desulfurization is in the removal of the decomposition products of thiophene (C_xH_y fragments and S) from these surfaces. At a temperature of 450 K, it is possible to hydrogenate and remove the C_xH_y fragments present on the $Ni_2P(001)$ surface [15]. On the other hand, the removal of the S adatoms ($S_{ads} + H_{2,gas} \rightarrow H_2S_{gas}$) is significant only at temperatures above 600 K [15]. Arrhenius plots obtained after measuring the hydrogenation rates at different temperatures (450, 500, 600 and 650 K) give *apparent* activation energies of 19-21 kcal/mol (0.8-0.9 eV) for the removal of S and 7-9 kcal/mol (0.3-0.4 eV) for the removal of the C_xH_y fragments. When similar experiments were done for the α-$Mo_2C(001)$ surface, again it was found that the most difficult step in a HDS process should be the transformation of adsorbed sulfur into gaseous H_2S [15]. In fact, at a temperature of 650 K, it was impossible to remove most of the S adsorbed on α-$Mo_2C(001)$.

In the rest of this section, we will focus our attention on the interaction S with the carbide and phosphide surfaces. The DF results displayed in Figure 3b indicate that MC(001) surfaces bind sulfur much weaker than $M_2C(001)$ surfaces (M= Ti, V or Mo) [16]. Experimental and theoretical results indicate that the S adsorbed on the MC(001) substrates interacts with the C sites in structural configurations similar to those seen for adsorbed oxygen (see Figure 5) [15,35]. A M→C charge transfer reduces the reactivity of the metal sites in MC compounds [2,3], and the S is forced to interact with the C sites which are not simple spectators. On the other hand, the $M_2C(001)$ surfaces bond strongly small and large coverages of sulfur [11,15,16]. These carbide systems have a reactivity towards S similar to that of pure metal surfaces [16]. For S/α-$Mo_2C(001)$, one doublet at 164-160 eV is detected in S 2p XPS spectra and does not change when the sample is heated at temperatures above 700 K [15].

In the case of S/$Ni_2P(001)$, two types of S species were seen in the S 2p XPS region: A set of two doublets appearing at 165-162 eV and 164-160 eV [15]. At small coverages of S only the doublet at 164-160 eV was found, and the sulfur was strongly bound remaining on the phosphide surface upon annealing to temperatures as high as 700 K. The results of DF calculations indicate that the S adtoms were probably sitting on the Ni hollow sites of $Ni_2P(001)$, see left-side panel in Figure 10 [15]. When the sulfur coverage was raised, there was a clear change in the line-shape of the S 2p features and the doublet at 165-162 eV appeared. The sulfur species that produced this doublet desorbed upon heating to 400-450 K. This "weakly" bound sulfur could be attached to Ni *and/or* P sites, since it induced a significant change in the line shape of the P 2p XPS spectrum for the phosphide substrate [15]. DF calculations show that Ni-P bridge sites are probably populated at medium or large sulfur coverages, see right side panel in Figure 10, and do

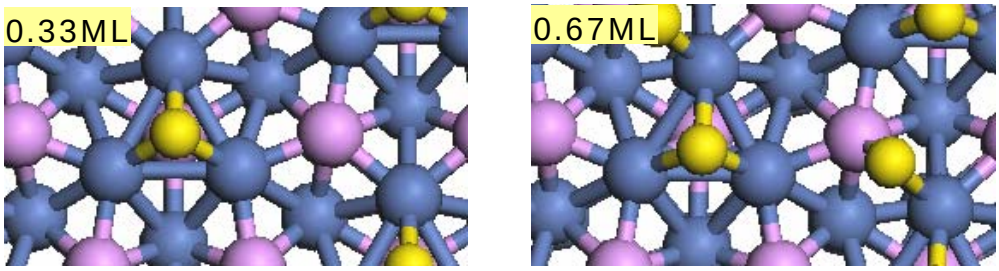

Figure 10 Bonding configurations calculated for 0.33 and 0.67 ML of atomic S on $Ni_2P(001)$. The dark blue spheres denote Ni atoms, while the soft purple spheres denote P atoms (taken from ref. [15]).

not interact strongly with the adsorbate. This Ni-P adsorption sites are interesting since they allow the participation of P atoms in hydrodesulfurization reactions.

Figure 11 compares the rates for removal of moderate to small coverages of sulfur from $Ni_2P(001)$ and α-$Mo_2C(001)$. Initially, approximately the same amount of sulfur was deposited on both surfaces, and then they were exposed to H_2 (500 Torr) at high temperature (650 K) [15]. The $H_{2,gas} + S_{ads} \rightarrow H_2S_{gas}$ reaction proceeds faster on $Ni_2P(001)$. In fact, only a very small amount of sulfur is removed from α-$Mo_2C(001)$. DF calculations give a barrier of ~ 4 eV for the hydrogenation of S on α-$Mo_2C(001)$ due to the extremely strong sulfur-surface bonds [15]. The

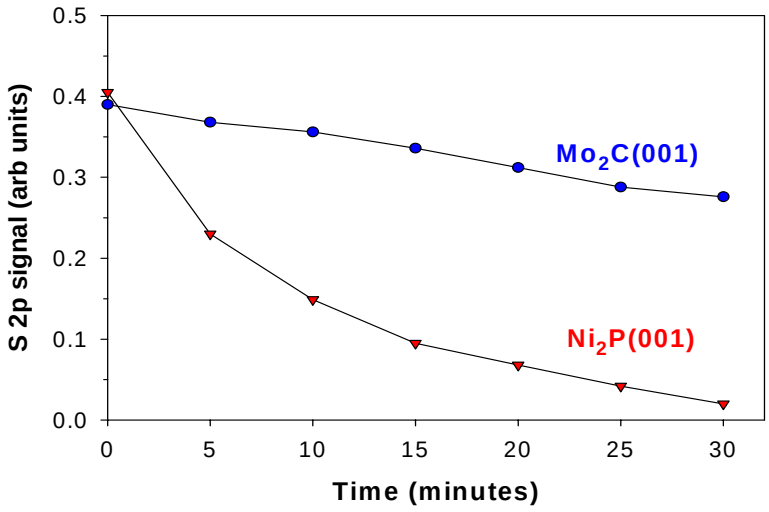

Figure 11 Hydrogenation of S adatoms on $Ni_2P(001)$ and α-$Mo_2C(001)$. Initially, approximately the same amount of sulfur was deposited on both surfaces. Then, the samples were exposed to H_2 (500 Torr) at 650 K. The removal of S was followed by measuring the changes in the S 2p XPS signal as a function of reaction time (taken from ref. [15]).

degradation of β-Mo_2C catalysts in desulfurization processes has been attributed to the formation of a chemisorbed layer of sulfur or MoS_xC_y compounds on the surface of these systems [31,32]. This is not the case for Ni_2P catalysts, which exhibit high stability with time [9,32,33].

The very good catalytic performance reported for Ni_2P [9,32,33] can be ascribed to the moderate effects of Ni↔P interactions and the intrinsic reactivity of the P sites [15]. First of all, the "ligand effect" of P atoms on the Ni sites is relatively weak. The formation of Ni-P bonds produces a minor stabilization of the Ni 3d levels and the Ni→P charge transfer is very small. This leads to a reasonably high activity of Ni_2P to dissociate thiophene and hydrogen. Secondly, the active Ni sites of the surface decrease due to an "ensemble effect" of P, which prevents the system from the deactivation induced by high coverages of strongly bound S. In addition, P sites play an important role in the bonding of intermediates. When the Ni hollow sites are occupied by an adsorbate, the P sites can provide moderate bonding to the products of the decomposition of thiophene and the H adatoms necessary for hydrogenation [15].

Ni_2P is a highly active HDS catalyst by obeying Sabatier's principle: good bonding with the reactants, and moderate bonding with the products. Bulk metal carbides like Mo_2C and MoC are not as good HDS catalysts because one interacts too strongly with the products (Mo_2C) and the other has problems dissociating the reactants (MoC) [15]. The DF results in Figure 3 indicate that the M_8C_{12} carbides have an intermediate reactivity between those of bulk Mo_2C and bulk MoC. Theoretical studies predict that Mo_8C_{12} and Ti_8C_{12} will be good HDS catalysts [17]. Figure 12 shows optimized structures for the reaction: thiophene + $3H_2$ → C_4H_8 + H_2S, on a Ti_8C_{12} metcar. Steps 1 to 8 are all exothermic and release the energy necessary for steps 9, 11 and 12 [17]. The rate determining step for the whole HDS process is the hydrogenation of adsorbed SH

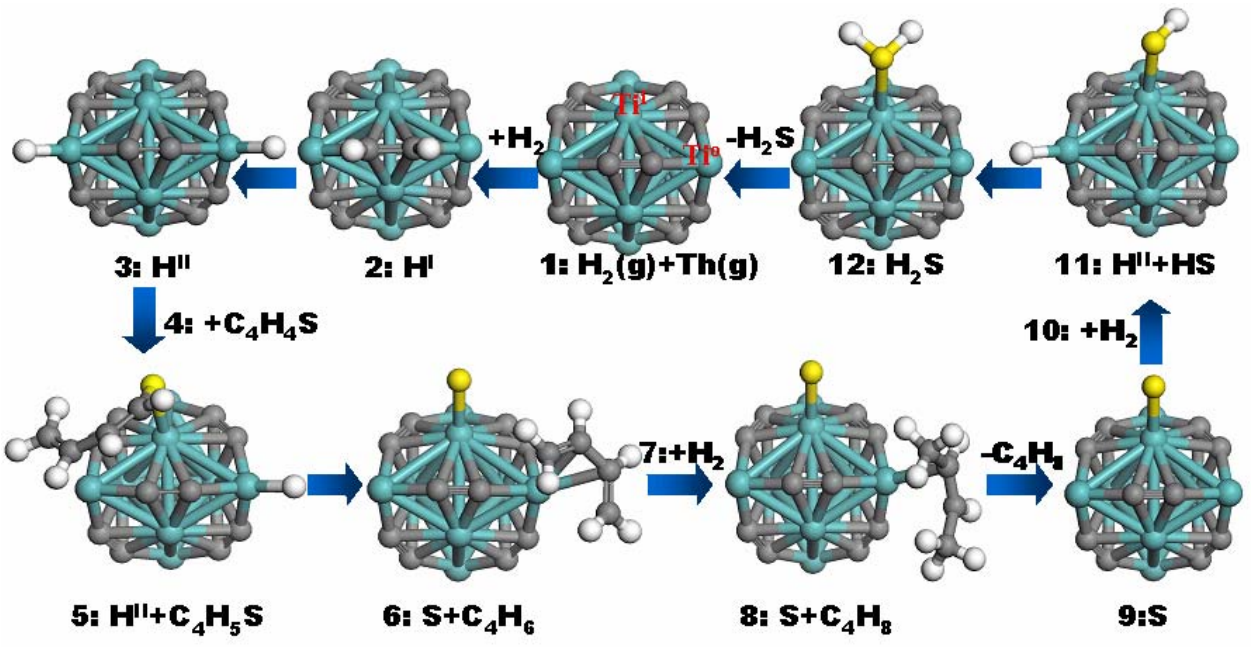

Figure 12 Optimized structures for the reaction: thiophene + $3H_2$ → C_4H_8 + H_2S, on a Ti_8C_{12} metcar. Blue spheres: Ti, grey spheres: C, white spheres: H, and yellow spheres: S (taken from ref. [17]).

(step 12) and subsequent evolution into gas phase of H_2S. On Ti_8C_{12} and Mo_8C_{12}, this step has an activation barrier smaller than on commercial Ni/MoS_2 catalysts [17]. In Figure 12, the dissociation of the first H_2 molecule takes place on the C_2 units of the metcar. The H adatoms are essential for the hydrogenolysis of the C-S bond in thiophene. In the absence of the H adtoms, the thiophene molecule just bonds to Ti_8C_{12} without any C-S bond breaking [16,36].

V. Conclusions

Transition metal carbides and phosphides have shown tremendous potential as highly active catalysts. Their high catalytic activity is usually attributed to ligand or ensemble effects. Recent studies reveal that the C and P sites in these compounds cannot be considered as simple spectators. They moderate the reactivity of the metal centers and provide bonding sites for adsorbates. The reactivity of the C centers in MC(001) surfaces varies in a complex way with the position of the metal in the Periodic Table and the filling of the carbide valence band. M_8C_{12} metcars should display a catalytic performance even better than that of the well-known Mo_2C or

MC catalysts. By introducing six pairs of C_2 groups in the structure, the M_8C_{12} system is stabilized, while the presence of four low-coordinated M sites allows a reasonable high chemical reactivity.

Acknowledgement

The research carried out at Brookhaven National Laboratory was supported by the US Department of Energy (Chemical Sciences Division, DE-AC02-98CH10886). F.V. thanks the Spanish Ministry of Education and Science (MEC, grants CTQ2005-08459-CO2-01, UNBA05-33-001) and Universitat de Barcelona for supporting his pre-doctoral research.

REFERENCES

1. J.G. Chen, Carbide and Nitride Overlayers on Early Transition Metal Surfaces Preparation, Characterization, and Reactivities, Chem. Rev. 96 (1996) 1477.
2. P. Liu, J.A. Rodriguez, Effects of Carbon on the Stability and Chemical Performance of Transition Metal Carbides: A Density Functional Study, J. Chem. Phys. 120 (2004) 5414.
3. F. Viñes, C. Sousa, P. Liu, J.A. Rodriguez, F. Illas, A Systematic Density Functiona Theory Study of the Electronic Structure of Bulk and (001) Surface of Transition-Metals Carbides, J. Chem. Phys. 122 (2005) 174709.
4. R.B. Levy, M. Boudart, Science, Platinum-Like Behavior of Tungsten Carbide in Surface Catalysis, 181 (1973) 547.
5. J.B. Claridge, A.P.E. York, A.J. Brungs, C. Marquez-Alvarez, J. Sloan, S.C. Tsang, M.L.H. Green, New Catalysts for the Conversion of Methane to Synthesis Gas: Molybdenum and Tungsten Carbide, J. Catal. 180 (1998) 85.

6. A.J. Brungs, A.P.E. York, M.L.H. Green, Comparison of the Group V and VI Transition Metal Carbides for Methane Dry Reforming and Thermodynamic Prediction of their Relative Stabilities, Catal. Lett. 57 (1999) 65.

7. R.R. Chianelli, G. Berhault, Symmetrical Synergism and the Role of Carbon in Transition Metal Sulfide Catalytic Materials, Catal. Today, 53 (1999) 357.

8. P. Liu, Interaction of Sulfur Dioxide with Titanium-Carbide Nanoparticles and Surfaces: A Density Functional Study, J.A. Rodriguez, J. Chem. Phys. 119 (2003) 10895.

9. S.T. Oyama, Preparation and Catalytic Properties of Transition-Metal Carbides and Nitrides, Catal. Today, 15 (1992) 179.

10. J.A. Rodriguez, J. Dvorak, T. Jirsak, J. Phys. Chem. B, 104 (2000) 11515.

11. T.P. St. Clair, S.T. Oyama, D.F. Cox, Adsorption and Reaction of Thiophene on Alpha-Mo_2C(0001), Surf. Sci. 511 (2002) 294.

12. P. Liu, J.A. Rodriguez, J.T. Muckerman, The Ti_8C_{12} Metcar: A New Model Catalyst for Hydrodesulfurization, J. Phys. Chem. B, 108 (2004) 15662.

13. L.E. Toth, *Transition Metal Carbides and Nitrides*, vol. 7 of *Refractory Materials* (Academic, New York, 1971).

14. E.K. Storms, *The Refractory Carbides* (Academic, New York, 1967).

15. P. Liu, J.A. Rodriguez, T. Asakura, J. Gomes, K. Nakamura, Desulfurization Reactions on Ni_2P(001) and α-Mo_2C(001) Surfaces: Complex Role of P and C Sites, J. Phys. Chem. B, 109 (2005) 4575.

16. P. Liu, J.A. Rodriguez, J.T. Muckerman, The Chemical Activity of Metal Compound Nanoparticles: Importance of Electronic and Steric Effects in M_8C_{12} (M= Ti, V, Mo) Metcars, J. Chem. Phys. 121 (2004) 10321.

17. P. Liu, J.A. Rodriguez, J.T. Muckerman, The Ti_8C_{12} Metcar: A New Model Catalyst for Hydrodesulfurization. J. Phys. Chem. B, 108 (2004) 18796.

18. D.J. Sajkowski, S.T. Oyama, Catalytic hydrotreating by molybdenum carbide and nitride: Unsupported Mo_2N and Mo_2C/Al_2O_3 Appl. Catal. A, 134 (1996) 339.

19. P. Frantz, S.V. Didziulis, Detailed Spectroscopic Studies of Oxygen on Metal Carbide Surfaces, Surf. Sci. 412/413 (1998) 384.

20. R. Souda, T. Aizawa, S. Otani, and Y. Ishizawa, Oxygen-Chemisorption on Transition-Metal Carbide (100) Surfaces Studied by X-Ray Photoelectron-Spectroscopy and Low-Energy He^+ Scattering, Surf. Sci. 256 (1991) 19.

21. K. Edamoto, T. Anazawa, E. Miyazaki and S. Otani, Chemisorption State of Atomic Oxygen on TiC(100) Surface - Angle-Resolved Photoemission-Study, Surf. Sci. 287 (1993) 667.

22. L.I. Johansson, H.I. Johansson, and K.L. Hakansson, Surface-Shifted N 1S And C 1S Levels on The (100) Surface of TIN and TIC, Phys. Rev. B, 48 (1993) 14520.

23. J.A. Rodriguez, P. Liu, J. Dvorak, T. Jirsak, J. Gomes, Y. Takahashi, and K. Nakamura, The Interaction of Oxygen with TiC(001): Photoemission and First-Principles Studies, J. Chem. Phys. 121 (2004) 465.

24. J.A. Rodriguez, P. Liu, J. Gomes, K. Nakamura, F. Viñes, C. Sousa, F. Illas, Interaction of Oxygen with ZrC(001) and VC(001): Photoemission and First-Principles Studies, Phys. Rev. B, 72 (2005) 075427.

25. Y.F. Zhang, F. Viñes, Y.J. Xu, Y. Li, J.Q. Li, F. Illas, Role of Kinetics in the Selective Surface Oxidations of Transition Metal Carbides, J. Phys. Chem. B, 110 (2006) 15454.

26. F. Viñes, C. Sousa, P. Liu, J.A. Rodriguez, F. Illas, Density Functional Study of the Adsorption of Atomic Oxygen on the (001) Surface of Early Transition-Metal Carbides, J. Phys. Chem. C, 111 (2007) 1307.

27. F. Viñes, C. Sousa, F. Illas, P. Liu, J.A. Rodriguez, A Systematic Density Functional Study of Molecular Oxygen Adsorption and Dissociation on the (001) Surface of Group IV, V and VI Transition Metal Carbides, submitted.

28. A.D. Becke, K.E. Edgecombe, A Simple Measure of Electron Localization in Atomic and Molecular-Systems, J. Chem. Phys. 92 (1990) 5397.

29. J.A. Rodriguez, J. Hrbek, Interaction of Sulfur with Well-Defined Metal and Oxide Surfaces: Unraveling the Mysteries behind Catalyst Poisoning and Desulfurization, Acc. Chem. Res. 32 (1999) 719.

30. E. Furimsky, Metal Carbides and Nitrides as Potential Catalysts for Hydroprocessing, Applied Catal. A: General, 240 (2003) 1.

31. B. Diaz, S.J. Sawhill, D.H. Bale, R. Main, D.C. Phillips, S. Korlann, R. Self, M.E. Bussell, Hydrodesulfurization over Supported Monometallic, Bimetallic and Promoted Carbide and Nitride Catalysts, Catal. Today, 86 (2003) 191.

32. K.A. Layman, M.E. Bussell, Infrared Spectroscopic Investigation of Thiophene Adsorption on Silica-Supported Nickel Phosphide Catalysts, J. Phys. Chem. B, 108 (2004) 15791.

33. J.A. Rodriguez, J.Y. Kim. J.C. Hanson. S.J. Sawhill, M.E. Bussell, Physical and Chemical Properties of MoP, Ni_2P, and MoNiP Hydrodesulfurization Catalysts: Time-Resolved X-Ray Diffraction, Density Functional, and Hydrodesulfurization Activity Studies, J. Phys. Chem. B, 107 (2003) 6276.

34. D. Kanama, S.T. Oyama, S. Otani, D.F. Cox, Photoemission and LEED Characterization of $Ni_2P(0001)$, Surf. Sci. 552 (2004) 8.

35. J.A. Rodriguez, P. Liu, J. Dvorak, T. Jirsak, J. Gomes, Y. Takahashi, K. Nakamura, Adsorption of Sulfur on TiC(001): Photoemission and First-Principles Studies, Phys. Rev. B, 69 (2004) 115414.

36. P. Liu, J.M. Lightstone, M.J. Patterson, J.A. Rodriguez, J.T. Muckerman, M.G. White, Gas-phase Interaction of Thiophene with $Ti_8C_{12}^+$ and Ti_8C_{12} Metcar Clusters. J. Phys. Chem. B, 110 (2006) 7449.